Measurements of IP3 and P1dB for Spectrum Monitoring with Software Defined Radios

Mike McNulty*†, Dazhen Gu†, Daniel G. Kuester†, Payam Nayeri*
*Colorado School of Mines, Golden, CO, US, mmcnulty@mines.edu, pnayeri@mines.edu
†National Institute of Standards and Technology, Boulder, CO, US, dazhen.gu@nist.gov, daniel.kuester@nist.gov

***Abstract*—This paper discusses methodology for characterizing linearity summary parameters of software-defined radio receivers. First, we introduce a highly automated testbed for 1-dB compression point (P1dB) and third-order input-intercept point (IIP3). With this system, we have observed some surprising deviations from the expected slope of 3 dB/dB in the power response of the third-order intermodulation distortion (IMD3). In response to this, we developed a measurement technique based on linear regression that accounts for the actual slope. A methodology study considers this technique in comparison with an existing technique for IIP3 measurements of spectrum monitoring receivers. In consideration for the increase in IMD3 model complexity, we also propose an alternative parameter to simplify the quantitative evaluation of spectral regrowth near the receiver noise floor. We argue that this equivalence point provides a designer with more valuable information than an IIP3 point for spectrum monitoring applications.**

I. Introduction

Software-defined radios (SDRs) are flexible, programmable transceivers that find increasing use in spectrum measurements. Like other transceivers, they are susceptible to nonlinearities that can cause spectral regrowth. This behavior needs to be characterized in order to quantify their efficacy in spectrum measurements. Yet, this is often difficult, because most SDR radio front-ends and digitizers are tightly integrated, sometimes just one or two chips on a circuit board.

It is common for manufacturers to provide detailed specification data on these front-end parameters in datasheets for the transceiver ICs, for example [1]. Unfortunately, it is much more difficult to find data on fully assembled SDRs, which is needed to capture the impacts of front-end amplification and filtering, as well as firmware-controlled transceiver configuration and calibration parameters. With this in mind, we decided to take a fresh look at measurement of SDR linearity in the context of spectrum measurement.

The paper lays out our exploratory study out as follows. Section II presents related literature and their contributions. Section III introduces a novel testbed designed to characterize SDRs. It also describes an original method to measure the third-order input intercept point (IP3) and one dB compression point (P1dB) of an SDR and compares it to an existing method presented by the International Telecommunication Union (ITU). Finally, Section IV examines the results of a test to characterize the IIP3 and P1dB of a USRP B200-mini at two center frequencies and multiple gain settings.

II. Related Work

A. Summary Parameters

Engineers most often summarize RF receiver linearity performance with the P1dB and IIP3 figures of merit. The principal reason that IMD3 products receive the greatest attention is that they tend to produce output distortion with the greatest power at the lowest level of input power [2]. These products are most likely to cause problems for (1) receivers operating in channels that are freuqency-adjacent to a powerful transmission, or (2) wideband or spectrum monitoring receivers that simultaneously receive powerful signals in two different bands (or channels).

Two-tone IIP3 testing is the most common way to evaluate the IMD3 properties of a DUT. The tones can be injected either inside or outside of the band of interest, in order to understand receiver blocking characteristics at different tone spacings [3]. The ITU recommends test procedures for manufacturers to test IIP3 in spectrum monitoring receivers [4]. They recommend obtaining IIP3 values under a wide range of conditions. The IIP3 specification from the DUT is then the lowest, "worst-case" result across the tested range of conditions.

B. Application to SDRs

Other authors have investigated various properties of commercial SDRs using automation platforms. Their efforts include characterizing the transmitted power versus output frequency and gain. Using this data they were able to produce an empirical model to describe the results [5]. Galal et al. [6] evaluated the tuning time versus tuning setting to find settings that met hopping requirements for multiple communications protocols. Zitouni et al. [7] compared the advertised frequency bandwidth and the true frequency bandwidth. They found that the measured bandwith was smaller than the advertised bandwidth. Corum et al. [8] measured the phase error between multiple SDRs used in a sensor network and used these measurements to correct the phase error.

Our literature review did not find any authors investigating various receiver characteristics such as the P1dB and IIP3 at different SDR settings. This motivated us to begin the experimental study that follows.

III. Testbed

1) Instrumentation: As an example of a widely-available consumer product, we undertook testing on an Ettus USRP

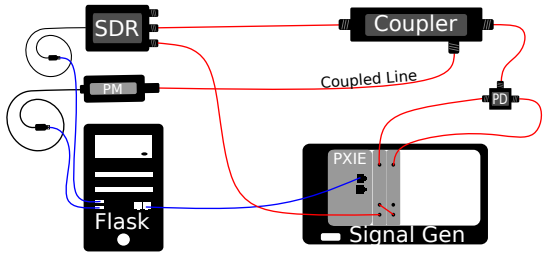

Fig. 1. Experimental setup.

B200-mini. The test hardware comprised two independent RF continuous-wave signal generators, an RF average power sensor, a two-way resistive power splitter, and a directional coupler. Together, test hardware supported 300 MHz – 6.6 GHz (limited by the coupler at the low end), covering most of the SDR tuning range, 10 MHz – 6 GHz. The power sensor measured the average power of the input signals at the coupled arm of the coupler and SDR RX to the output. Reference outputs from the signal generators reference outputs synchronized baseband time and LO phase in the USRP. A schematic illustrates this in Fig. 1.

2) Automation: To characterize the operating characteristics of an SDR, a test platform was developed to control the SDR and the instruments. We used GNURadio [9] as a software abstraction to automate a wide range of SDRs, including USRP Hardware Driver (UHD). Additionally, because the test setup required multiple workstations, the platform needed the ability to communicate with network connected devices. Flask [10] is a WSGI web application framework that provided HTTP endpoints for automation of each device.

The test software consisted of three components: the choreographer, generator devices, and data acquisition devices. The choreographer was a single piece of software that maintained the states of all of the generators and data acquisition devices on the test platform. The choreographer for this study was designed using a python Flask server. Its function was to execute the test procedure by performing operations for each device in the proper sequence. The test procedure can be repreated for a set of parameters, which comprise the settings for the generator and SDR data acquisition. In addition to endpoints required to maintain orchestration, the flask server provided an easy HTTP interface to monitor the state of a test and reset the platform.

The three primary endpoints implemented by the choreographer were the individual state request (ISR), group state request (GSR), and the parameters request. The ISR was an HTTP POST request and allowed each device to update its state on the server. Each time the ISR endpoint was accessed, the sever checked the other devices' states to see if they were in a common state. If either group (generators, data

Certain commercial equipment, instruments, or materials are identified in this paper in order to specify the experimental procedure adequately. Such identification is not intended to imply recommendation or endorsement by NIST, nor is it intended to imply that the materials or equipment identified are necessarily the best available for the purpose.

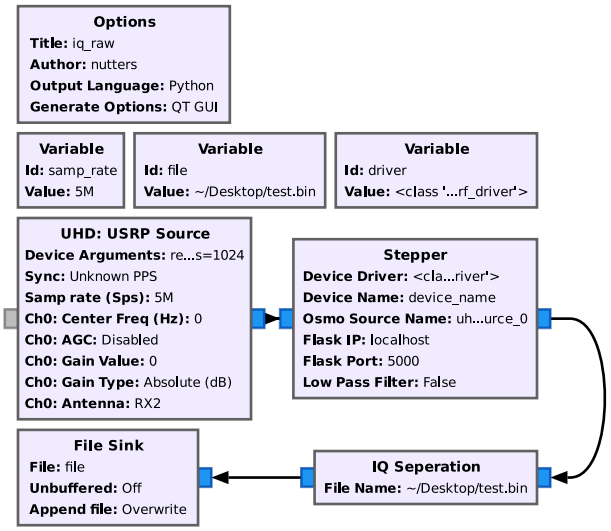

Fig. 2. GNURadio flow-graph for acquisition of IQ waveforms.

acquisition) was in a common state, the server updated that group's status to reflect the shared state.

The "group state request" was implemented as an HTTP GET. This endpoint provided the status of the entire system (running or finished), the status of the generators (ready, transmitting, or done), and the status of the data acquisition devices (ready, reading, or done) in JSON format.

The last endpoint was the "parameters endpoint," represented as a JSON file. The current parameter incremented when every device on the test platform posted a "done" state to the (ISR) endpoint. The check for "done" was carried out every time a device requested the parameter endpoint.

The SDR was automated using GNURadio. A single GNURadio block, designated the "stepper," was used to manage the SDR's settings and inform downstream blocks about the parameter settings used to collect the samples. The stepper began collecting samples once all generators indicated "transmitting." During the settling period, a user-defined number of samples were discarded. Following the settling period, the stepper moved to the dwell period where the first sample was marked with a "start" tag and additional tags for each setting returned by the parameter request. Once the user-defined number of dwell samples were collected, the stepper marked the final sample with an "end" tag. Finally, the stepper waited for a new parameter to be supplied by the Flask server, and the process would repeat until samples for all parameters were captured.

The stepper was designed with real-time data processing in mind, although all the data collected for this paper was raw in-phase and quadrature (IQ) data. A GNURadio block "IQ Separation" was designed to manage the output file of the file sink block. The file sink block takes a file name as an input parameter and allows the user to update the file name in real-time. Each time the IQ Separation block received an end tag, a new file was created to allow for easy identification of each test parameter. The file name contained a trailing number that

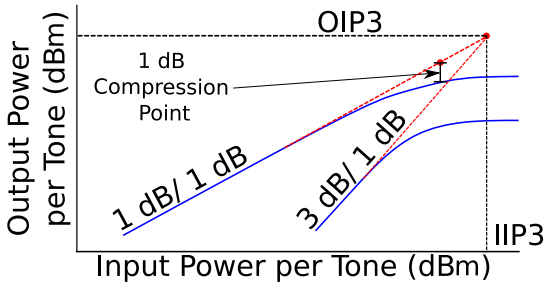

Fig. 3. Underlying model of summary parameters for receiver linearity.

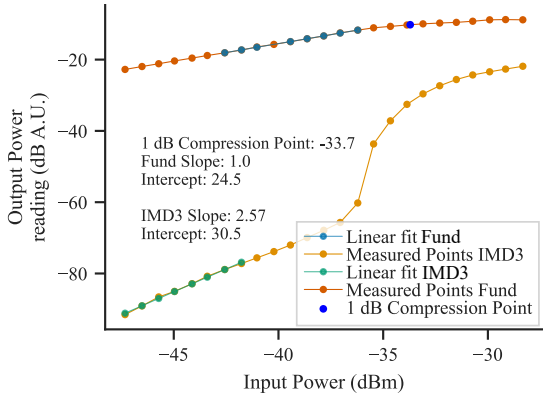

Fig. 4. In-band power response of the DUT at 40 dB gain, measured at 701.5 MHz.

was incremented with each successive parameter until a folder was full of files for each parameter. Figure 2 shows the simple flowgraph that was used to collect the SDR data.

A. Baseband Power Spectrum

We estimated the power spectral density (PSD) per tone in the baseband following Welch's method [11]. This power spectrum estimate is a result of fast Fourier transforms (FFTs) of overlapping windowed time domain waveforms, and applying power averaging. The first step was to acquire a discrete complex-valued time series of 5×10^6 long. This was split into 76 FFT windows of length 2^{16} samples, before Blackman-Harris windows were applied. The uncalibrated output power spectrum was determined by the bin-wise average of linear power across the 76 modified periodograms, with no time overlap.

B. Fundamental Tones

We refer to the two input tones together as the fundamental. The average input power per tone was measured from power sensor, de-embedded with S-parameter measurements to the network plane at the SDR input; output power was determined from the PSD. To determine P1dB, we used a linear regression to establish the ideal linear response, following Fig. 3. This was the reference used to estimate the 1-dB compression value.

C. Third-Order Intermodulation Measurements

We focused in some detail on IIP3 test methodology. In doing so, we considered an alternative measurement technique, which is compared here with ITU method.

1) ITU Method: The existing ITU recommendation, for comparison, is to compute IIP3 from test data as

$$\text{IIP3 (ITU)} = P_{in} + \frac{a}{2}. \tag{1}$$

Here, P_{in} is the average power per input tone in dBm, and a is the ratio of output power at the strongest IIP3 tones to the average at the input tones in dB. This measurement is to be repeated across a range of different test conditions, including input tone frequency separations, P_{in} values, center frequencies, and physical temperatures.

TABLE I
BASEBAND FREQUENCIES UNDER TEST

	In-band		Out-of-band	
	Freq. (MHz)	Bin	Freq. (MHz)	Bin
Fundamental f_1	0.504	6604	1001.000	N/A
Fundamental f_2	1.000	13108	2001.992	N/A
IMD3 $f_{3,1}$	0.008	100	0.008	100
IMD3 $f_{3,2}$	1.496	19612	3002.984	N/A

2) Proposed Method: The general approach here was to extrapolate IIP3 through statistical regression of the power response of the fundamental and IMD3 tones. Our starting assumption was that the slopes of these regression lines would match those in Fig. 3, at least at low power levels. Thus, in order to avoid errors at the edges of dynamic range, we limited the domain of the fit to the range of input power levels that produced output slope nearest to 1 dB/dB or 3 dB/dB. This was performed by minimizing the mean-squared error in the slope. This was performed for each SDR {sample rate, settling time}.

Some experimental data demonstrating this procedure is illustrated by Fig. 4. A surprising aspect of this response is that the slope of the IMD3 power response was not 3 dB/dB. To extrapolate the intercept point, we used the slope, though this has implications on the application of IIP3 (see Section IV).

The same test data can also be used to determine the 1 dB-compression point of the device. Under the same subset of input power levels as with IIP3, the P1dB was calculated by locating the 1-dB drop in output power compared to the linear regression. The output power between measurement points was estimated using a cubic interpolation function [12]. Both IIP3 and P1dB specifications are graphically explained in Fig. 3.

IV. Example Measurements

To demonstrate the test system and compare the IIP3 measurement techniques, we performed some preliminary experiments on an Ettus USRP B200-mini. In these tests, the SDR was operated with {sample rate = 5 Msps, settling time = 0.3 s, dwell time = 1.0 s}. There were two frequency configu-

TABLE II
ONE- AND TWO-TONE MEASUREMENT DATA

			RX gain setting in the DUT						
			0.0	10.0	20.0	30.0	40.0	50.0	
701.5 MHz	In-band	Fund. intercept	-12.6	-4.2	5.5	15.6	24.5	34.4	dBAU
		Fund. RMSE	0.0	0.0	0.0	0.0	0.0	0.1	dB
		IMD3 slope	2.7	2.9	2.7	2.7	2.6	2.3	dB/dB
		IMD3 intercept	-26.6	-15.6	-12.0	11.3	30.5	39.8	dBAU
		IMD3 RMSE	0.1	0.6	0.1	0.9	0.6	0.4	dB
		P1dB	N/A	-4.4	-14.6	-25.0	-33.7	-43.8	dBm
		IIP3 (proposed)	8.0	5.9	10.4	2.5	-3.8	-4.1	dBm
		IIP3 (ITU)	4.7	4.8	4.8	-3.3	-12.6	-20.1	dBm
		N Intersect	-37.0	-37.4	-41.6	-48.3	-58.7	-65.8	dBm
	Out-of-Band	Fund. intercept	-8.2	0.0	9.6	19.9	28.7	38.5	dBAU
		Fund. RMSE	0.2	0.0	0.0	0.0	0.0	0.1	dB
		IMD3 slope	2.4	3.7	3.0	3.0	3.0	2.9	dB/dB
		IMD3 intercept	-49.5	-23.9	-16.6	-3.6	35.3	43.0	dBAU
		IMD3 RMSE	0.3	5.9	0.4	0.2	0.2	0.0	dB
		IIP3 (proposed)	29.2	8.9	13.1	11.7	-3.3	-2.3	dBm
		IIP3 (ITU)	15.0	17.9	13.1	11.1	-3.4	-4.4	dBm
		N Intersect	-32.3	-27.3	-35.5	-38.5	-51.9	-52.5	dBm
2437 MHz	In-band	Fund. intercept	-16.6	-8.5	1.1	10.4	20.9	30.6	dBAU
		Fund. RMSE	0.0	0.0	0.1	0.0	0.0	0.0	dB
		IMD3 slope	2.7	2.7	2.7	2.4	2.9	2.8	dB/dB
		IMD3 intercept	-37.4	-29.8	-15.3	-1.9	44.8	2.8	dBAU
		IMD3 RMSE	1.1	0.4	0.0	1.2	0.1	0.2	dB
		P1dB	N/A	N/A	-10.4	-19.8	-30.2	-39.4	dBm
		IIP3 (proposed)	12.5	12.6	9.5	8.5	-12.7	-11.8	dBm
		IIP3 (ITU)	7.6	8.6	5.7	-2.0	-14.4	-20.4	dBm
		N Intersect	-33.7	-35.1	-39.3	-48.1	-57.6	-62.4	dBm
	Out-of-Band	Fund. intercept	-12.4	-4.3	5.2	14.3	24.8	34.5	dBAU
		Fund. RMSE	0.1	0.1	0.1	0.0	0.0	0.0	dB
		IMD3 slope	2.4	3.5	3.0	3.0	3.0	3.0	dB/dB
		IMD3 intercept	-58.6	-38.6	-28.0	-16.5	24.4	33.7	dBAU
		IMD3 RMSE	0.3	2.9	2.8	0.1	0.1	0.0	dB
		IIP3 (proposed)	33.2	13.8	16.6	15.4	0.2	0.4	dBm
		IIP3 (ITU)	18.2	20.4	16.6	15.1	0.1	-0.4	dBm
		N Intersect	-28.6	-24.5	-31.5	-34.4	-48.7	-49.1	dBm

TABLE III
MEASUREMENT PARAMETER KEY

Fund. intercept	Linear fit intercept for fundamental tones ("gain")
Fund. RMSE	Linear fit RMSE in fundamental tones
IMD3 slope	Response slope for IMD3 tones
IMD3 intercept	Intercept for IMD3 tones
IMD3 RMSE	RMSE for IMD3 tones

(a) Regression parameters of the linear fit to output power

P1dB	Input power at 1 dB compression
IIP3 (proposed)	Input IP3 with the proposed technique
IIP3 (ITU)	Input IP3 with the ITU method
N Intersect	Fund. input power at IMD3 $= kTB$

(b) Measurands

rations in these tests, "in-band" and "out-of-band," referring to the location of the input tones relative to the sampling band of the SDR. The specific frequencies and FFT bin indices (FFT size 2^{16}) of the fundamental and IMD3 tones in these tests are listed in Table I. These were selected to the frequencies of the input tones and IMD3 products at integer bins, maximizing frequency selectivity. For out-of-band tests, the slope of the fundamental was collected by injecting a single tone inside the sampling band after the IMD3 slope measurement. The wide out-of-band spacing was chosen to be significantly larger than the maximum sampling rate of the SDR.

Table II lists measurement data across frequency and gain setting. Uncalibrated power-proportional quantities are in dB relative to arbitrary units (dBAU). The goodness-of-fit for the linear fits is expressed here in terms of root-mean-squared error (RMSE). In most cases, the small errors suggested "good" fits, though some of the IMD3 fits (particularly out-of-band) were greater than 1 dB. The small-signal output power response of the fundamental tone was left out of Table II because all measurements were within 0.02 dB of 1 dB/dB. One of the most important observations is the large number of IMD3 responses that deviated from the 3 dB/dB slope. This phenomenon was most pronounced in-band tests and typically fell under the traditional prediction. Although this was not strictly the case, for example, the 701.5 MHz and 2437 MHz out-of-band tests at 10 dB gain produced IMD3 slopes of 3.69 dB/dB and 3.49 dB/dB, respectively.

The row "IIP3 (ITU)" gives the mean value of IIP3s computed with the ITU method at each input power level used in the IMD3 linear regression. Comparing this average to "IIP3 (proposed)" provides insight into the differences between the two IIP3 measurement techniques under ideal conditions when all of the measurement points fall in the most linear operating region of the SDR. Because most of the IMD3 linear regression slopes were smaller than 3 dB/dB, most of the IIP3 results from the proposed method predicted higher IIP3.

Figure 5 presents a comparison between results of the two types of IIP3 measurements. In contrast to Table II, the points labeled ITU IIP3 in Fig. 5 span all points collected inside and outside the bounds described in Subsection III-C2. The degree of agreement between the ITU and the proposed method is important to note because it could affect decision-making when selecting or operating an SDR. If a designer leverages IIP3 to estimate spectral regrowth from an adjacent channel, they may be surprised when the receiver under-performs if the IIP3 was measured under ITU guidance at high input power levels between -30 dBm and +10 dBm. Figure 6 shows the variation in the ITU's IMD3-noise equivalent point depending on the input power used. This indicates an IIP3 value may need to be accompanied by the slope of the IMD3 tones to estimate an upper bound on adjacent channel power in specifying SDR dynamic range.

To reduce dependence on IMD3 slope, we considered an alternative to IIP3, which is labeled in Tables II-III as N Intersect. This metric is the input power at which the IMD3 tones are equal to the receive thermal noise. The values

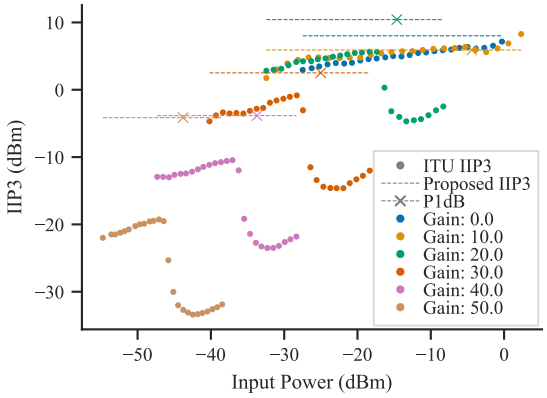

Fig. 5. 701.5 MHz in-band IIP3 comparison.

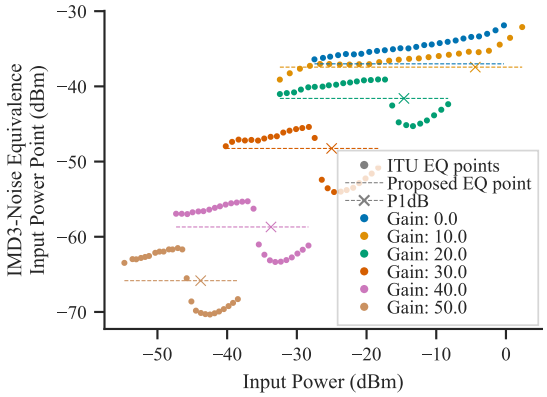

Fig. 6. 701.5 MHz in-band noise equivalence comparison.

shown were extrapolated with the regression parameters and receive noise power measurements. In other words, this is the input power level that results in a decrease of 3 dB in signal to interference-plus-noise ratio (SINR) in the band due to the IMD3 contribution. With this data and a reasonable estimate for the slope of IMD3 tones, the designer could estimate an input power limit based on application-specific SINR requirements.

V. Conclusion

This paper introduced an automated RF measurement testbed designed for extended one- and two-tone measurements of SDR receiver linearity. With this capability, we demonstrated an exploratory study on 1 dB compression point, and on IIP3 measurements performed with input tones located both inside and outside the SDR sampling bandwidth. The resulting insights are drawn from experiments by varying a large number of parameters thanks to the automation.

A surprising trend emerged from the test data: power in IMD3 tones with respect to the input power was not always 3 dB/dB, even at low input power levels. This slope is important, because it is used to extrapolate both upward to express IIP3, and downward to estimate maximum overload threshold levels in spectrum monitoring receivers. Because these linear extrapolations may easily span 10s of dBs of input power, seemingly-insignificant errors in the slope may be multiplied manifold in dB, leading to significantly inaccurate conclusions. As a result, the basic definition of IIP3 illustrated in Fig. 3 no longer applies, calling into question both the basic meaning and the applicability of IIP3 in the SDR receiver.

In response to this unexpectedly complex IMD3 behavior, we considered alternative metrics that may be better suited. First, we considered specifying the small-signal slope of the IMD3, and accounting for it in calculating IIP3. This can apply when the small-signal IMD3 power response slope is linear; measurements are similar to the ITU method, but with more input power sampling points. Additionally, we considered how the IMD3 performance of the receiver could be expressed instead in terms of the 2-tone power level that drives IMD3 products to equal the noise power in the band. We argue that a noise intersection point like this is more general, because it gives immediate insights into practical receiver operation, but with fewer assumptions about the non-linear device characteristics.

Extension of this work could lead to more general test methodologies. For instance, testing a wider variety of SDRs with different architectures would help to identify whether the observed behaviors are typical. Testing based on communications and radar modulation would also offer a path toward connecting these insights with link budget parameters. Further, an uncertainty analysis would help stakeholders in frequency selectivity measurements to interpret the reliability of compression and IMD3 measurements.

References

[1] *RF Agile Transceiver AD9364*, Analog Devices. [Online]. Available: https://www.analog.com/media/en/technical-documentation/data-sheets/AD9364.pdf

[2] S. A. Maas, *Nonlinear microwave and RF circuits*. Artech house, 2003.

[3] *IIP3 Measurements*, Analog Devices, June 2018. [Online]. Available: https://ez.analog.com/wide-band-rf-transceivers/design-support/w/documents/10070/out-of-band-and-in-band-iip3-measurements

[4] *Test procedure for measuring the 3rd order intercept point (IP3) level of radio monitoring receivers*, International telecommunication Union, August 2013. [Online]. Available: https://www.itu.int/dms_pubrec/itu-r/rec/sm/R-REC-SM.1837-1-201308-I!!PDF-E.pdf

[5] R. Zitouni and S. Ataman, "An empirical model of the sbx daughter board output power driven by usrp n210 and gnu radio based software defined radio," in *2015 IEEE 12th International Multi-Conference on Systems, Signals Devices (SSD15)*, 2015, pp. 1–5.

[6] I. Galal, M. E. A. Ibrahim, and H. E. Ahmed, "Exploring frequency tuning policies for usrp-n210 sdr platform and gnu radio," in *2013 Conference on Design and Architectures for Signal and Image Processing*, 2013, pp. 298–303.

[7] R. Zitouni, S. Ataman, and L. George, "RF measurements of the rfx 900 and rfx 2400 daughter boards with the usrp n210 driven by the gnu radio software," in *2013 International Conference on Cyber-Enabled Distributed Computing and Knowledge Discovery*, 2013, pp. 490–494.

[8] S. Corum, J. D. Bonior, R. C. Qiu, N. Guo, and Z. Hu, "Evaluation of phase error in a software-defined radio network testbed," in *2012 Proceedings of IEEE Southeastcon*, 2012, pp. 1–4.

[9] GNU Radio, *(accessed 2021-09)*. [Online]. Available: https://www.gnuradio.org/doc/doxygen/

[10] Pallets, *(accessed 2021-09)*. [Online]. Available: https://flask.palletsprojects.com/en/2.0.x/

[11] M. Proakis, *Digital signal processing: principles algorithms and applications*. Pearson Prentice Hall, 2001.

[12] interp1d. SciPy, *(accessed 2021-09)*. [Online]. Available: https://docs.scipy.org/doc/scipy/reference/reference/generated/scipy.interpolate.interp1d.html#scipy.interpolate.interp1d